Electronic Supplementary Material (ESI) for Analytical Methods.

Supplemental Methods and Data

A Nuclease Protection ELISA Assay for Colorimetric and Electrochemical Detection of Nucleic Acid

Jessica E. Filer[1,2], Robert B. Channon[3], Charles S. Henry[3,4*], Brian J. Geiss[1,4*]

[1]Department of Microbiology, Immunology, and Pathology, Colorado State University, Fort Collins, CO 80523, USA

[2]Cell and Molecular Biology Graduate Program, Colorado State University, Fort Collins, CO 80523, USA

[3]Department of Chemistry, Colorado State University, Fort Collins, CO 80523, USA

[4]School of Biomedical Engineering, Colorado State University, Fort Collins, CO 80523, USA

S1.1 Electrochemical Characterization of Hydroquinone/Benzoquinone and 3,3',5,5'-Tetramethylbenzidine

Horseradish peroxidase (HRP) catalyzes the reduction of peroxide into water using a cosubstrate that functions as an electron donor. The two-electron oxidation of 3,3',5,5'-Tetramethylbenzidine (TMB) into its yellow product (ox2-TMB) by HRP is described in the main text. Although TMB is the most widely used as an HRP substrate due to its chromogenic properties, multiple other molecules can function as an HRP substrate including hydroquinone (HQ), o-phenilendiamine, p-chlorophenol, and more [1]. Due to its widespread use in biosensor applications [2–6], HQ was chosen as a second electrochemical substrate to compare against TMB. HQ also undergoes a two-electron oxidation to form its product p-benzoquinone (BQ) via a semiquinone intermediate [7]. To determine the optimal electrode material for analysis, cyclic voltammetry (CV) was performed with both enzymatic products (1 mM BQ in 1× PBS, pH 7.4 and ox2-TMB in proprietary citrate buffer + H_2SO_4, pH 1) using Au (2 mm diameter) and glassy carbon electrodes (GCE) (3 mm), as well as a Pt electrode (2 mm) to test BQ (Fig S1). BQ exhibits one reduction peak at 0.115 V for Au, 0.036 V for GCE, and 0.067 V for Pt and a single oxidation peak at 0.179 V, 0.315 V, and 0.304 V respectively. Peak to peak values (ΔE_p) are shown in Table 1 and are graphed in Fig S1b. The ΔE_p for GCE and Pt are large at 279 mV and 237 mV respectively, indicating a quasi-reversible process / slow electron transfer kinetics. ΔE_p for Au,

however, was close to ideal at 64 mV and suggests that the BQ reduction to HQ is reversible at an Au electrode. The Au working electrode was thus chosen for further HQ-BQ analysis.

Table 1. Peak to peak separation of BQ CV curves

Electrode Metal	ΔE_p (mV)
Au	64
GCE	279
Pt	237

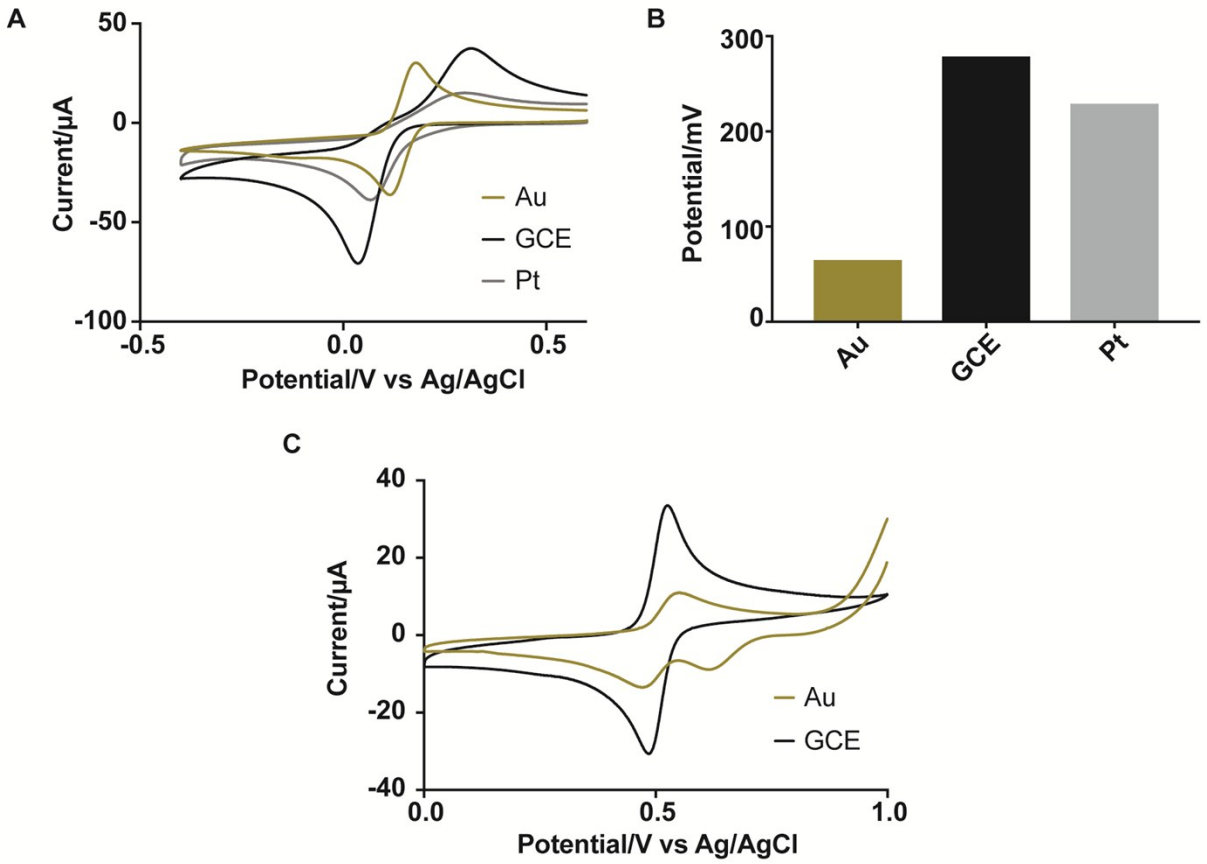

Fig S1. Electrode optimization for BQ and TMB analysis. a) Cyclic voltammetry of 1 mM BQ in 1× PBS (pH 7.4) with Au, GCE, and Pt electrodes. b) ΔE_p values for BQ CV analysis with Au, GCE, and Pt electrodes. c) Cyclic voltammetry of ox2-TMB in proprietary citrate buffer + H_2SO_4 (pH 1) with Au and GCE electrodes.

Interestingly, the redox behavior of ox2-TMB was different at Au and GCE electrodes. At the Au electrode, ox2-TMB exhibits two reduction peaks at 0.615 V and 0.473 V but only a single

oxidation peak at 0.549 V. Conversely for GCE, there is one reduction peak at 0.486 V and one oxidation peak at 0.525 V. The ΔE_p for GCE was 39 mV, which suggests that the species readily adsorbs to the carbon surface [8]. This was also evidenced by extensive fouling as depicted in Fig S2. Although fouling was also noted for both BQ and TMB at the gold electrode, it was less pronounced. To mitigate the effects of fouling, the Au electrode was polished with alumina slurry then washed with Milli Q water in between all measurements and was used for downstream TMB analysis.

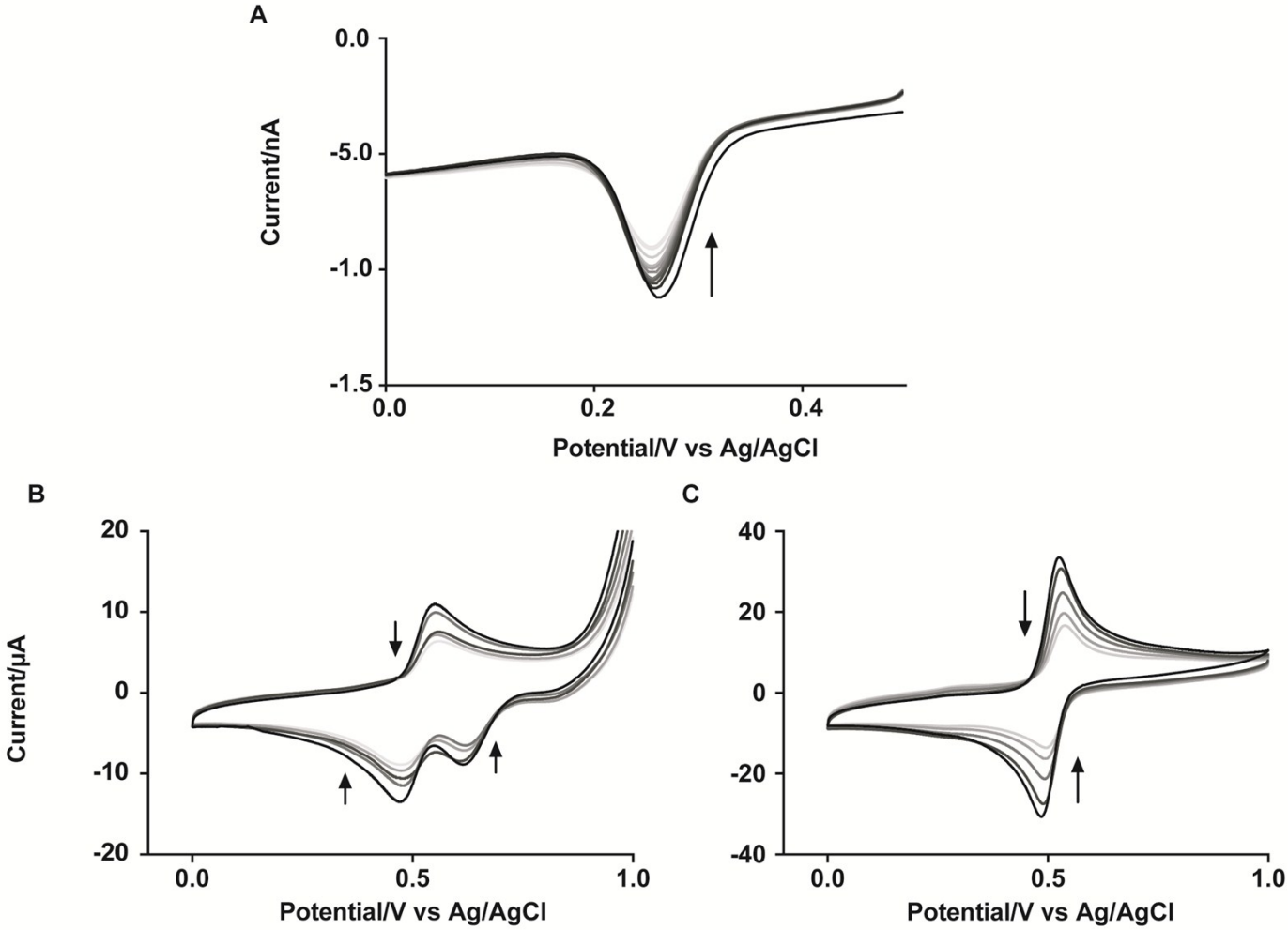

Fig S2. Electrode fouling during BQ and TMB analysis. a) Repeated square wave voltammetry measurements of 1mM BQ in H_2SO_4 with Au electrode. b) Repeated cyclic voltammetry measurements of ox2-TMB in proprietary citrate buffer + H_2SO_4 (pH 1) with Au electrode. c) Repeated cyclic voltammetry measurements of ox2-TMB in proprietary citrate buffer + H_2SO_4 (pH 1) with GCE electrode.

Electrochemical characterization of the HRP substrates and products was performed using cyclic voltammetry and the results are shown in Fig S3. 1 mM HQ and 1 mM BQ in 1× PBS were tested and compared in Fig S3a. HQ exhibited oxidation and reduction peaks at 0.241 V and 0.071 V respectively with a ΔE_p of 170 mV, which is indicative of an irreversible process. BQ however, showed oxidation and reduction peaks at 0.179 V and 0.115 V with a ΔE_p of 64 mV. It is not clear what leads to irreversible electrochemical behavior for HQ but not BQ. Furthermore, BQ exhibited a second small reduction peak at -0.133 V which could correspond to the semiquinone intermediate and was not observed at the GCE and Pt electrodes.

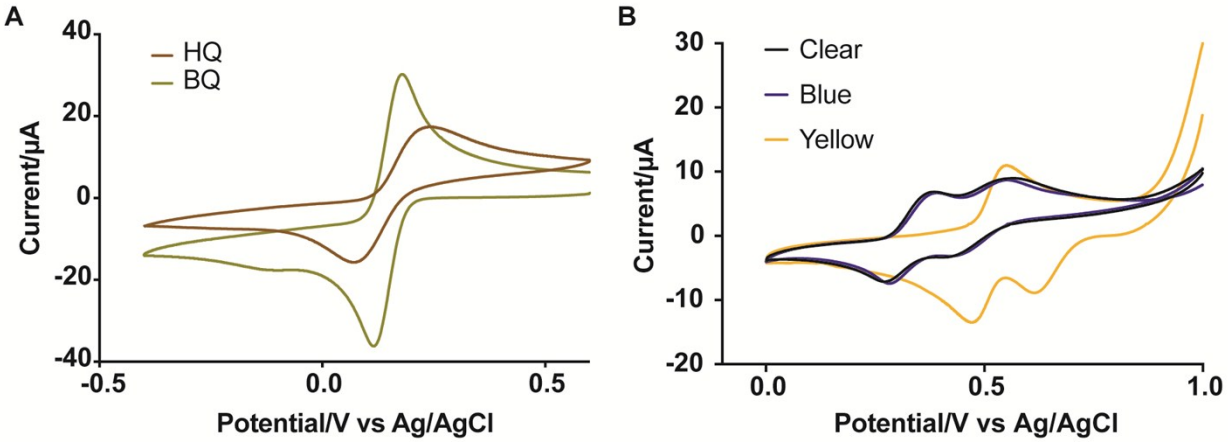

Fig S3. Electrochemical characterization of HRP substrates and products. a) Cyclic voltammetry of 1 mM HQ and 1 mM BQ in 1× PBS. b) Cyclic voltammetry of TMB (clear species) and ox1-TMB (blue species) in proprietary citrate buffer and ox2-TMB (yellow species) in citrate buffer + H_2SO_4 (pH 1).

Next, the electrochemical behavior of TMB was analyzed in a 1-Step TMB-Ultra solution from ThermoScientific (Fig S3b). The clear species exhibited two oxidation peaks at 0.606 V and 0.412 V as well as two reduction peaks at 0.439 V and 0.267 V. The blue species (ox1-TMB) was generated by adding 50μL of 200 pg mL^{-1} anti-Digoxigenin/HRP in 1× PBS to 900μL of clear TMB substrate. It behaved similarly with two oxidation peaks at 0.563 V and 0.384 V and two reduction peaks at 0.418 V and 0.273 V. Because the yellow species (ox2-TMB) is only stable at low pH, it was generated by adding 100μL of 8 M H_2SO_4 to the solution and it demonstrated different electrochemical behavior. Likely due to the lower pH, the two reduction peaks were shifted towards higher potentials at 0.615 V and 0.473 V. Only a single oxidation peak was noted at 0.549 V and is likely due to the instability of the TMB intermediate form at low pH.

Due to its speed and sensitivity, square wave voltammetry was used for assay analysis as described in the main text. Initial potential ($E_{initial}$) was optimized for BQ analysis as shown in Fig S4a. A small relationship between $E_{initial}$ and peak current (i_p) was observed. Starting the scan at higher potentials may convert extra HQ to BQ before being converted back to HQ during reduction. Thus, starting at higher potentials has a small signal amplification effect. Scan frequency was also optimized as shown in Fig S4b. Higher frequencies generate a larger signal but may also correspond to higher capacitive background signal. The signal to noise ratios are listed in Table 2 and were largest for 15 Hz (3.05) which was chosen for further analysis.

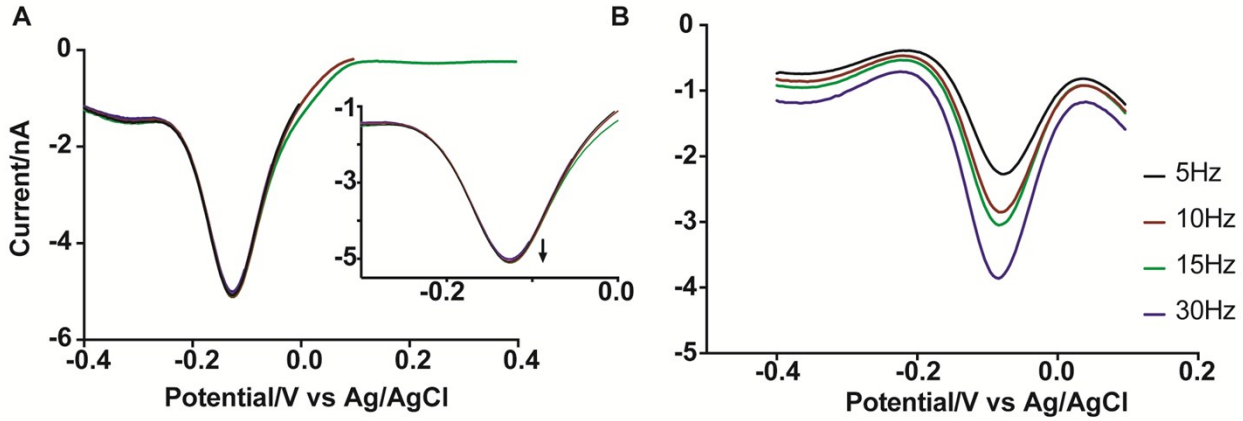

Fig S4. Optimization of square wave voltammetry parameters. a) Relationship between initial potential ($E_{initial}$) and peak current (i_p) during square wave voltammetry analysis of 1 mM BQ in 1× PBS. b) Relationship between frequency and current response during square wave voltammetry analysis of 5 mM HQ + 100 µM BQ in 1× PBS.

Table 2. Relationship between frequency and signal to noise ratio for square wave voltammetry

Frequency (Hz)	S/N
30	2.99
15	3.05
10	3.01
5	2.71

References

[1] S. V. Kergaravat, M.I. Pividori, S.R. Hernandez, Evaluation of seven cosubstrates in the quantification of horseradish peroxidase enzyme by square wave voltammetry, Talanta. 88 (2012) 468–476. doi:10.1016/j.talanta.2011.11.016.

[2] W. Hong, S. Lee, Y. Cho, Dual-responsive immunosensor that combines colorimetric recognition and electrochemical response for ultrasensitive detection of cancer biomarkers, Biosens. Bioelectron. 86 (2016) 920–926. doi:10.1016/j.bios.2016.07.014.

[3] H. Wang, Q. Rong, Z. Ma, Polyhydroquinone-graphene composite as new redox species for sensitive electrochemical detection of cytokeratins antigen 21-1, Nat. Publ. Gr. (2016) 1–6. doi:10.1038/srep30623.

[4] G. Martínez-García, E. Sánchez-Tirado, A. González-Cortés, P. Yáñez-Sedeño, J.M. Pingarrón, Amperometric immunoassay for the obesity biomarker amylin using a screen printed carbon electrode functionalized with an electropolymerized carboxylated polypyrrole, Microchim. Acta. 185 (2018) 323. doi:10.1007/s00604-018-2863-x.

[5] M. Giannetto, M.V. Bianchi, M. Mattarozzi, M. Careri, Competitive amperometric immunosensor for determination of p53 protein in urine with carbon nanotubes/gold nanoparticles screen-printed electrodes: A potential rapid and noninvasive screening tool for early diagnosis of urinary tract carcinoma, Anal. Chim. Acta. 991 (2017) 133–141. doi:10.1016/j.aca.2017.09.005.

[6] E. Sánchez-Tirado, G. Martínez-García, A. González-Cortés, P. Yáñez-Sedeño, J.M. Pingarrón, Electrochemical immunosensor for sensitive determination of transforming growth factor (TGF) - β1 in urine, Biosens. Bioelectron. (2016) 1–6. doi:10.1016/j.bios.2016.05.093.

[7] N. Akai, A. Kawai, K. Shibuya, Water assisted photo-oxidation from hydroquinone to p-benzoquinone in a solid Ne matrix, J. Photochem. Photobiol. A Chem. 223 (2011) 182–188. doi:10.1016/j.jphotochem.2011.08.016.

[8] A.J. Bard, L.R. Faulkner, Electrochemical methods: fundamentals and applications, 2nd ed., John Wiley & Sons, Inc., New York, 2001.